Modeling of Mature Soot Dynamics and Optical Properties

Georgios A. Kelesidis, Sotiris E. Pratsinis
Particle Technology Laboratory, ETH Zurich, Zurich, Switzerland

Aleksandar Duric, Martin Allemann
Siemens Schweiz AG, Building Technologies Division, Zug, Switzerland

Abstract

Agglomeration and surface growth of fractal-like soot nanoparticles are investigated by Discrete Element Modeling (DEM) to elucidate the effects of primary particle polydispersity and chemical bonding (aggregation) on soot morphology and optical properties. The Discrete Dipole Approximation (DDA) is used to estimate the differential, $dC_{sca}/d\Omega$, and integral scattering cross sections, C_{sca}, of soot agglomerates of aggregates and spheres. The DDA calculations are validated against the $dC_{sca}/d\Omega$ values predicted by Mie theory and measured from monodisperse polystyrene spheres, attaining maximum deviations of 22 and 16 %, respectively.

Agglomerates of polydisperse aggregates and spheres produced by agglomeration and surface growth have more compact structure and larger fractal dimension, D_f, than agglomerates consisting of monodisperse spheres. The evolution of D_f from nascent to mature soot by agglomeration and surface growth is in excellent agreement with microscopic measurements in premixed and diffusion flames. Primary particle polydispersity and aggregation enhance the $dC_{sca}/d\Omega$ and C_{sca} of DEM-derived agglomerates up to 50 and 30 %, respectively. This indicates the need to account for the complex agglomerate morphology in the calculations of soot optical properties for the optimization of fire detectors.

Keywords: light scattering, fractal dimension, soot, fire detection modeling

Introduction

Most of today's fire detectors work by light scattering of soot particles generated in open and smoldering fires. To optimize fire detectors and improve quantitative measurement of soot emissions, soot radiative properties have to be determined accurately. Thus, the effect of the complex particle morphology on soot optical properties has to be understood in depth.

Soot particles are typically in the form of fractal-like agglomerates, consisting of polydisperse primary particles physically or chemically bonded together (aggregates) by surface growth after their inception and during their coagulation. Soot can be classified in two categories based on its formation stage, namely nascent (particles of 1-50 nm mobility diameter) and mature soot (fractal-like agglomerates with mobility diameters between 50 and 1000 nm). Aggregation by acetylene surface reaction is crucial during nascent soot growth, forming compact structures with fractal dimension, D_f larger than 2 [1,2]. Mature soot agglomerates sampled from combustion engines [3] and diffusion flames [4] have D_f of 1.8 ± 0.2.

Traditionally the optical properties of soot have been approximated with the well-known and relatively easy-to-use Mie theory for spheres, neglecting the fractal-like nature of soot. The Rayleigh-Debye-Gans (RDG) theory for agglomerates consisting of primary particles in point contact (e.g. bonded by physical forces) has been applied alternatively, resulting in better agreement with optical measurements in both open and smoldering fires than Mie theory using different refractive indexes [5]. However, RDG is unable to resolve the effect of overlapping soot primary particles typically observed in microscopic images of soot. The robust Discrete Dipole Approximation (DDA) has been validated against RDG for the case of agglomerates of spheres [6]. However, the chemical bonding induced by surface growth has either been neglected or assumed uniform for all primary particles neglecting their polydispersity [7].

Here, soot dynamics by agglomeration and surface growth are quantified by Discrete Element Modeling (DEM). The evolution of soot morphology from nascent to mature agglomerates is quantified by D_f and compared to microscopic measurements from premixed [1] and diffusion flames [4]. The mature soot differential, $dC_{sca}/d\Omega$, and integral scattering cross sections, C_{sca}, are estimated by DDA. The DDA calculations are validated against Mie theory and measurements of monodisperse polystyrene spheres. The scattering properties of DEM-derived mature soot agglomerates of polydisperse aggregates and spheres are compared to those of agglomerates of monodisperse spheres.

Numerical Implementation

The dynamics of soot growing by coagulation with surface growth after inception are described by DEM, accounting for Brownian and neglecting van der Waals, electric or hydrodynamic forces [2]. Here, two hundred monodisperse soot particles with initial particle diameter, $d_{p,o}$ = 2 nm are randomly distributed in a cubic cell at 1 atm and 1830 K applying periodic boundary conditions [2].

The Hydrogen Abstraction Carbon Addition (HACA) mechanism [8] is used to model surface growth. The initial number of hydrogen atoms that

generate the surface radicals for HACA is calculated from the soot mass balance to attain a mean primary particle diameter, $\bar{d}_p$, of 15 nm. When acetylene molecules collide with either single particles or primary particles within aggregates or agglomerates, they react increasing the particle mass by two carbon atoms [8] and forming chemical bonds between primary particles (aggregation). The increase of (primary) particle diameter is estimated by a mass balance [2].

Every collision between particles is successful and leads to formation of a new cluster. The time between particle collisions is calculated by an event-driven method [9]. The evolution of agglomerate morphology consisting of monodisperse spheres with $\bar{d}_p$ = 15 nm was obtained similarly to Goudeli et al. [9].

The gyration, d_g, mobility, d_m, volume-equivalent, d_v, and primary particle diameters, d_p, are calculated for each agglomerate in the cubic cell. The evolutions of the different mean agglomerate diameters are derived as function of time [2]. The fractal-like agglomerate morphology is characterized by the fractal dimension, D_f, that relates the agglomerate mass, m_a, to d_g by [2]:

$$m_a \sim d_g^{D_f} \qquad \text{(Eq. 1)}$$

Optical Properties Calculations

The DDA is used here to calculate the light scattering of DEM-derived agglomerates of aggregates and/or spheres. The DDA calculations are done using the open-source DDSCAT 7.3 code [10]. The fractal-like agglomerate morphology is represented on a lattice by an array of discrete dipoles interacting with each other through their electric fields [10]. The Maxwell's equations are discretized on the lattice using the volume-integral equation method and subsequently solved iteratively [10]. The dipole spacing, d, must be small compared to the incident light wavelength, λ, to calculate accurately the differential scattering cross section, $dC_{sca}/d\Omega$. This accuracy criterion is quantified by the relation $k|m|d < 0.5$, where m is the material's refractive index and $k = 2\pi/\lambda$ [10]. The $dC_{sca}/d\Omega$ is estimated for incident and scattered light beams horizontally-polarized with respect to the scattering plane by [10]:

$$\frac{dC_{sca}}{d\Omega} = \frac{1}{2k^2}\left(S_{11} + S_{12} + S_{21} + S_{22}\right) \qquad \text{(Eq. 2)}$$

where S_{11}, S_{12}, S_{21} and S_{22} are the DDA-derived Mueller's matrix elements. The integral scattering cross section, C_{sca}, is obtained by the scattering efficiency, Q_{sca} [10]:

$$C_{sca} = Q_{sca}\frac{\pi}{4}d_v^2 \qquad \text{(Eq. 3)}$$

DDA Validation

Figure 1 shows the DDA-estimated differential scattering cross section, $dC_{sca}/d\Omega$ (Equation 2), of monodisperse polystyrene spheres with 989 nm diameter as function of the scattering angle, θ, using $k|m|d$ of 0.48 (dotted line), 0.25 (dot-broken line) and 0.12 (solid line). For the applied incident light wavelength, λ, of 690 nm, the polystyrene refractive index, $m = 1.586$ was chosen [11]. The DDA-derived $dC_{sca}/d\Omega$ is compared to those predicted from Mie theory (broken line) and measured (diamonds) by Loepfe et al. [11]. All $k|m|d$ values shown in Figure 1 are smaller than the limit of 0.5, required for accurate DDA calculations [2], and result in almost identical $dC_{sca}/d\Omega$ distributions. The DDA accuracy increases for smaller $k|m|d$ [10]. As $k|m|d$ decreases from 0.48 (dotted line) to 0.25 (dot-broken line), the maximum deviation from $k|m|d = 0.12$ (solid line) is reduced from 20 to 6 % at θ = 180°. Lower $k|m|d$ values result in less than 2 % difference from $k|m|d = 0.12$ (solid line).

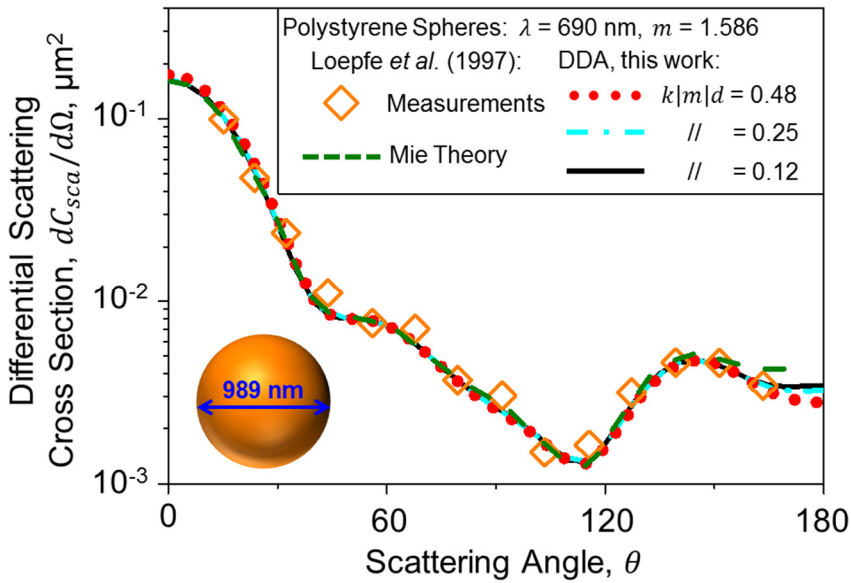

Fig. 1. DDA-estimated $dC_{sca}/d\Omega$ of monodisperse polystyrene spheres as function of θ using different $k|m|d$ (dotted, dot-broken and solid lines). The DDA-derived $d\sigma_{sca}/d\Omega$ is compared to those measured (diamonds) and estimated using the Mie theory (broken line) by Loepfe et al. [11].

The DDA calculations for $k|m|d$ = 0.12 (solid line) underestimate the $dC_{sca}/d\Omega$ measured (diamonds) and estimated by Mie theory (broken line) up to 16 and 22 %, respectively, at θ = 90 and 180°, respectively. This underestimation can be attributed to the slight polydispersity of the polystyrene spheres produced by Loepfe et al. [11] that is not accounted for in this work. The Mie theory (broken line) overestimates the measured

$dC_{sca}/d\Omega$ (diamonds) up to 24 % at θ = 165°. The DDA-calculations with $k|m|d$ = 0.12 (solid line) are in good agreement with Mie theory (broken line) and measurements (diamonds) and thus used in all DDA calculations henceforth. This $k|m|d$ is also below the stricter limit of 0.32 suggested for accurate DDA calculations of strongly absorbing soot nanoparticles [7].

DEM-derived Soot Morphology Evolution

Figure 2 shows the DEM-derived evolution of the fractal dimension, D_f (Equation 1), of soot agglomerates of polydisperse spheres and aggregates (solid line, red images) as function of the normalized mean mobility diameter, $\bar{d}_m$ / $\bar{d}_p$, that is increasing with time. The DEM-derived evolution of D_f is compared to that of agglomerates of monodisperse spheres (broken line, green images) and microscopic measurements of soot measured in premixed [1; squares, blue-framed image] and diffusion flames [4; triangles, orange-framed image].

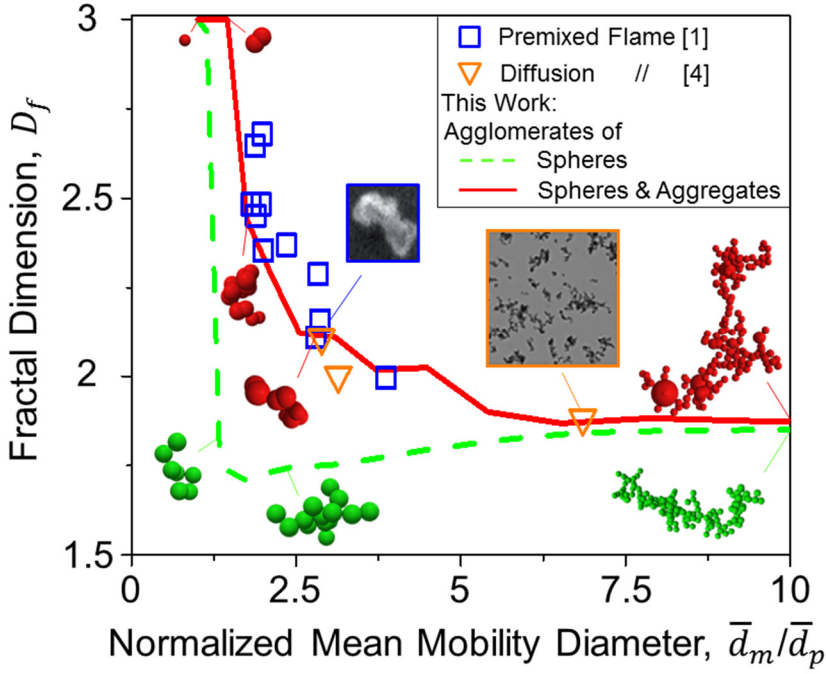

Fig. 2. DEM-derived evolution of D_f of soot agglomerates consisting of monodisperse spheres (broken line, green images) and polydisperse aggregates and spheres (solid line, red images) as function of the normalized mean mobility diameter, $\bar{d}_m$ / $\bar{d}_p$. The DEM-derived evolutions of D_f are compared to microscopic measurements in premixed [1; squares, blue-framed image] and diffusion flames [4; triangles, orange-framed image].

In the absence of surface growth (broken line, green images), ramified agglomerates of monodisperse spheres are produced by agglomeration only, attaining an asymptotic D_f of 1.85 ± 0.01 for $\bar{d}_m / \bar{d}_p > 6$. When surface growth takes place (solid line, red images), polydisperse aggregates and spheres are formed having more compact morphology and larger D_f than agglomerates of monodisperse spheres (broken line, green images). The DEM-derived evolution of D_f of agglomerates of aggregates and spheres is in good agreement with microscopic measurements of soot in premixed [1; squares, blue-framed image] and diffusion flames [4; triangles, orange-framed image], confirming that aggregation by surface growth determines largely nascent soot formation for $\bar{d}_m / \bar{d}_p$ up to 5 [2]. Surface growth stops for $\bar{d}_m / \bar{d}_p > 5$ and coagulation of the formed aggregates and spheres decreases D_f down to an asymptotic 1.87 ± 0.02. The DEM-derived asymptotic D_f is in good agreement with theory [9] and microscopic measurements of mature soot in diffusion flames [4; triangles, orange-framed image].

Light Scattering by Mature Soot Agglomerates

Figure 3 shows the DDA-derived $dC_{sca}/d\Omega$ (Equation 2) of two representative mature soot agglomerates with d_m = 150 nm, consisting of polydisperse aggregates and spheres (solid line, red image) or monodisperse spheres (broken line, green image). Both agglomerates were sampled from the respective DEM-derived populations with mean $\bar{d}_m / \bar{d}_p = 10$, shown in Figure 2. The DDA calculations were done for λ = 405 nm and m = 1.48+0.84i [12] as function of θ. The agglomerate $dC_{sca}/d\Omega$ has been averaged over 343 orientations. Sensitivity analysis showed that averaging over more than 343 agglomerate orientations results in less than 2 % difference in the estimated $dC_{sca}/d\Omega$, in agreement with DDA calculations [7].

Both agglomerate $dC_{sca}/d\Omega$ distributions have a peak at θ = 90°, in excellent agreement with theory [7]. The agglomerate $dC_{sca}/d\Omega$ for polydisperse aggregates and spheres (solid line, red image) is larger compared to that of monodisperse spheres (broken line, green image) due to its more compact structure (Figure 2). Even though the effect of aggregation and polydispersity on D_f is about 1 % for $\bar{d}_m / \bar{d}_p = 10$ (Figure 2), it results in 7 % larger volume-equivalent diameter, d_v, and 30 % larger integral scattering cross section, C_{sca} (Equation 3). The $dC_{sca}/d\Omega$ of simulated soot agglomerates at θ = 180° was enhanced by 33 % accounting for uniform chemical bonding between primary particles and by 25 % accounting for their polydispersity [7]. Here, both primary particle aggregation and polydispersity are accounted for resulting in 50 % increase of $dC_{sca}/d\Omega$ at θ = 180°.

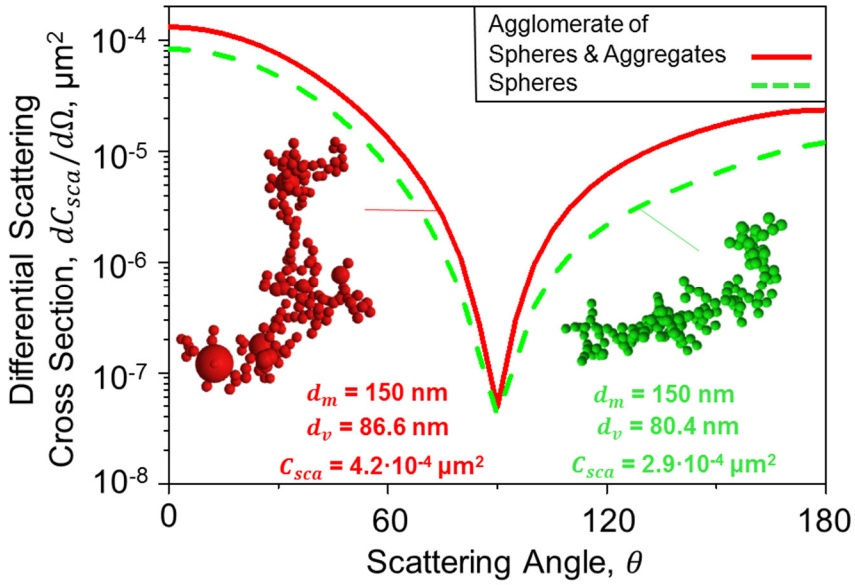

Fig. 3. DDA-estimated $dC_{sca}/d\Omega$ and C_{sca} of two representative soot agglomerates consisting of monodisperse spheres (broken line, green image) or polydisperse aggregates and spheres (solid line, red image). Both agglomerates were sampled from the respective DEM-derived populations with mean $\bar{d}_m / \bar{d}_p = 10$ shown in Figure 2.

Conclusions

The dynamics from nascent to mature fully-developed soot structures are investigated by Discrete Element Modeling (DEM) during agglomeration and surface growth. Primary particle aggregation and polydispersity induced by surface growth enhances the DEM-obtained evolution of fractal dimension, D_f, and significantly improves its agreement with microscopic measurements of soot nanoparticles produced in premixed [1] and diffusion flames [4].

The integral, C_{sca}, and differential scattering cross sections, $dC_{sca}/d\Omega$, of DEM-derived soot agglomerates are investigated using the Discrete Dipole Approximation (DDA). The DDA calculations are validated against Mie theory and measurements of monodisperse polystyrene spheres, attaining maximum deviations of 22 and 16 %, respectively. Agglomerates of polydisperse aggregates and spheres have up to 30 and 50 % larger C_{sca} and $dC_{sca}/d\Omega$, respectively, compared to agglomerates of monodisperse spheres. This indicates the need to account for both primary particle aggregation and polydispersity to simulate accurately soot morphology and optical properties and optimize fire detectors.

Acknowledgements

The research leading to these results has received partial funding from ETH Zurich (# ETH-08 14-2).

References

[1] M. Schenk et al., "*Imaging Nanocarbon Materials: Soot Particles in Flames are Not Structurally Homogeneous*", ChemPhysChem 13, 3248-3254, 2013.

[2] G.A. Kelesidis et al., "*Flame Synthesis of Functional Nanostructured Materials & Devices: Surface Growth & Aggregation*", Proceedings of the Combustion Institute 36, 29-50, 2017.

[3] A. Neer, U.O. Koylu, "*Effect of operating conditions on the size, morphology, and concentration of submicrometer particulates emitted from a diesel engine*", Combustion and Flame 146, 142-154, 2006.

[4] M.R. Kholghy et al., "*Comparison of multiple diagnostic techniques to study soot formation and morphology in a diffusion flame*", Combustion and Flame 176, 567-583, 2017.

[5] M. Loepfe et al., "*Application of the Rayleigh-Debye-Gans theory on the scattering of light by standard test fire aerosols*", AUBE14, 2014.

[6] A. Soewono, S.N. Rogak, "*Morphology and Optical Properties of Numerically Simulated Soot Aggregates*", Aerosol Science and Technology 47, 267-274, 2013.

[7] N. Doner, F. Liu, "*Impact of morphology on the radiative properties of fractal soot aggregates*", Journal of Quantitative Spectroscopy and Radiative Transfer 187, 10-19, 2017.

[8] J. Appel et al., "*Kinetic modeling of soot formation with detailed chemistry and physics: laminar premixed flames of C2 hydrocarbons*", Combustion and Flame 121, 122-136, 2000.

[9] E. Goudeli et al., "*Coagulation–Agglomeration of Fractal-like Particles: Structure and Self-Preserving Size Distribution*", Langmuir 31, 1320-1327, 2015.

[10] B.T. Draine, P.J. Flatau, "*Discrete-dipole approximation for scattering calculations*", Journal of the Optical Society of America A 11, 1491-1499, 1994.

[11] M. Loepfe et al., "*Optical properties of fire and non-fire aerosols*", Fire Safety Journal 29, 185-194, 1997.

[12] J. Yon et al., "*On the radiative properties of soot aggregates part 1: Necking and overlapping*", J Journal of Quantitative Spectroscopy and Radiative Transfer 162, 197-206, 2015.